ChemPlusChem

Research Article
doi.org/10.1002/cplu.202400025

Chemistry Europe
European Chemical Societies Publishing

www.chempluschem.org

Improved L-Asparaginase properties and reusability by immobilization onto functionalized carbon xerogels

Rita A. M. Barros[+,[a, b]] Raquel O. Cristóvão[+,[a, b]] Inês. G. Carneiro,[a, b] Maria A. Barros,[a, b] Matheus M. Pereira,[c] Sónia A. C. Carabineiro,[a, d] Mara G. Freire,[e] Joaquim L. Faria,[a, b] Valéria C. Santos-Ebinuma,[f] Ana P. M. Tavares,[e] and Cláudia G. Silva*[a, b]

Enzyme immobilization can offer a range of significant advantages, including reusability, and increased selectivity, stability, and activity. In this work, a central composite design (CCD) of experiments and response surface methodology (RSM) were used to study, for the first time, the L-asparaginase (ASNase) immobilization onto functionalized carbon xerogels (CXs). The best results were achieved using CXs obtained by hydrothermal oxidation with nitric acid and subsequent heat treatment in a nitrogen flow at 600 °C (CX–OX-600). Under the optimal conditions (81 min of contact time, pH 6.2 and 0.36 g/L of ASNase), an immobilization yield (*IY*) of 100 % and relative recovered activity (*RRA*) of 103 % were achieved. The kinetic parameters obtained also indicate a 1.25-fold increase in the affinity of ASNase towards the substrate after immobilization. Moreover, the immobilized enzyme retained 97 % of its initial activity after 6 consecutive reaction cycles. All these outcomes confirm the promising properties of functionalized CXs as support for ASNase, bringing new insights into the development of an efficient, and stable immobilization platform for use in the pharmaceutical industry, food industry, and biosensors.

1. Introduction

Nearly 1 out of 3 diagnoses of cancer in children and teenagers is leukemia, making it the most common form of this disease.[1]

[a] R. A. M. Barros,[+] R. O. Cristóvão,[+] I. G. Carneiro, M. A. Barros,
     S. A. C. Carabineiro, J. L. Faria, C. G. Silva
     LSRE-LCM – Laboratory of Separation and Reaction Engineering –
     Laboratory of Catalysis and Materials, Faculty of Engineering, University of
     Porto, Rua Dr. Roberto Frias, 4200-465 Porto, Portugal
     Tel: +351 220 414 874
     E-mail: cgsilva@fe.up.pt

[b] R. A. M. Barros,[+] R. O. Cristóvão,[+] I. G. Carneiro, M. A. Barros, J. L. Faria,
     C. G. Silva
     ALiCE – Associate Laboratory in Chemical Engineering, Faculty of
     Engineering, University of Porto, Rua Dr. Roberto Frias, 4200-465
     Porto, Portugal

[c] M. M. Pereira
     University of Coimbra, CIEPQPF, Department of Chemical Engineering, Rua
     Sílvio Lima, Pólo II – Pinhal de Marrocos, 3030-790 Coimbra, Portugal

[d] S. A. C. Carabineiro
     LAQV-REQUIMTE, Department of Chemistry, NOVA School of Science and
     Technology, Universidade NOVA de Lisboa, 2829-516 Caparica, Portugal

[e] M. G. Freire, A. P. M. Tavares
     CICECO-Aveiro Institute of Materials, Department of Chemistry, University of
     Aveiro, 3810-193 Aveiro, Portugal

[f] V. C. Santos-Ebinuma
     São Paulo State University (UNESP), School of Pharmaceutical Sciences,
     Department of Bioprocess Engineering and Biotechnology, Araraquara,
     Brazil

[+] These authors contributed equally to this work.

Unlike cancer in adults, most childhood cancers do not have a known cause and are acute, which means they develop rapidly.[2] It is the case of acute lymphoblastic leukemia (ALL), a form of blood cancer that rapidly spreads and affects white blood cells. With advances in the development of recombinant therapeutic enzymes, specifically L-asparaginase (ASNase), the long-term outcome of ALL has improved substantially over the last decades, with survival rates in children reaching 90 %[3] and 30–40 % in adults.[4] ASNase (E.C.3.5.1.1) is a tetrameric enzyme that catalyzes the hydrolysis of L-asparagine (L-Asn) into ammonium and L-aspartic acid (L-Asp).[5] In contrast to normal cells, leukemic ones lack or have little asparagine synthetase, being unable to produce L-Asn (an important amino acid for their proliferation).[6] As a result, by depriving malignant cells of this essential growth factor, ASNase causes cell death and has an antileukemic effect.[7,8] Additionally, ASNase is also used in the food industry to stop the Maillard reaction, which occurs mainly in starch-rich foods between reducing sugars and L-Asn at high temperatures[9] and results in the creation of acrylamide (a carcinogenic and toxic substance).[10] Besides, its use as a biosensor to detect L-Asn levels in both industries has also been reported.[11]

ASNase can be found in several animals, plants, and microorganisms (bacteria, fungi, algae).[12] However, the enzyme frequently employed in the management of ALL is derived from bacterial sources, specifically *Escherichia coli* (EcASNase II)[13] and *Erwinia chrysanthemi*.[14] Although progress in using ASNase is encouraging, its application faces certain challenges.[15] The widespread use of recombinant enzymes in the pharmaceutical industry is still affected by their high cost, primarily associated with the purification processes.[16] Besides, bacterial ASNase has a short half-life, and a fast plasma clearance, and has been associated with some adverse side effects.[17,18] Therefore, many researchers have been searching for novel microorganisms that

produce ASNase with fewer adverse effects,[19] and finding strategies to optimize the related purification methods.[20] Moreover, its unstable and thermolabile nature has also affected its use in the food industry.[21] As a result, by allowing their reuse over multiple cycles, the improvement of ASNase's stability can lead to a significant increase in catalytic efficiency and contribute to its affordability.

ASNase immobilization onto solid supports is a promising method used to overcome the problems associated with its use in the food and therapeutic fields.[22] Improved catalytic performance, tuned selectivity and specificity, reusability, resistance to different environmental factors and inhibitors, and easier separation are some of the main aims of enzyme immobilization in these fields.[23,24] If properly designed, immobilization can also be associated with enzyme purification.[25] Various solid supports, comprising organic, inorganic, and hybrid compounds, have been reported to immobilize ASNase.[26,27]

Carbon-based nanomaterials have gained significant attention as supports for enzymes due to their impressive physicochemical properties, such as large surface area and adsorption capacity, unique porous size and structure, and ability to introduce functional groups, all of which provide exciting features for the development of new biocatalytic processes.[28–32] Carbon gels present a promising and innovative class of carbon-based nanomaterials for immobilizing proteins.[33] These materials are synthesized through the carbonization of organic gels, formed by polymerizing resorcinol and formaldehyde in water using a basic catalyst to promote the reaction.[34] The drying method used determines the type of gel produced, with supercritical,[35] cryogenic,[36] or subcritical drying[37] resulting in aerogels, cryogels, or xerogels, respectively. Subcritical is the cheapest and fastest drying method available, which makes carbon xerogels (CXs) the best choice for large-scale production and application.[36] The most interesting particularity of these materials is their porous structure and controlled pore size distributions, which can be tailored with relatively high precision.[38]

Like with other carbon-based nanomaterials,[39] it is possible to change the surface chemistry of the CXs by increasing the number of oxygenated groups to enhance the surface reactivity and hydrophilicity. That is done by an oxidation treatment called functionalization in the gas or liquid phase.[40–43] HNO_3 is commonly used during the CXs functionalization due to its highly controllable oxidizing properties with temperature, concentration, and treatment duration changes.[44] Despite CX's promising properties, to the best of our knowledge, no study on the functionalization of these materials for ASNase immobilization has been reported in the scientific literature. Therefore, this study focuses on the immobilization of ASNase onto a new form of functionalized CXs, for the first time, as a tool to obtain an enhanced performance of the enzyme while contributing towards its sustainable use. Research in enzyme immobilization is still very much needed.[25] Our previous research demonstrated that a straightforward physical adsorption method can effectively immobilize ASNase onto pristine CXs.[45] While this approach showed great potential in terms of preserving ASNase

activity, the formation of stronger linkages between the support and the enzyme is extremely recommended since it normally results in bioconjugates with increased stability and reusability.[46] For this purpose, surface functionalization of CXs can be a promising solution.

In this work, CXs functionalized by hydrothermal oxidation with nitric acid and subsequent treatment at different temperatures were studied for the first time in the immobilization of commercial *E. coli* ASNase by simple physical adsorption. To achieve maximum immobilization yield (*IY*) and enzyme relative recovered activity (*RRA*), the immobilization conditions were optimized by testing various contact times, pH values, and enzyme concentrations. For this, an in-depth experimental central composite design (CCD) and response surface methodology (RSM) were used. Additionally, the immobilized ASNase operational, and storage stabilities were tested, and the kinetic parameters were obtained.

2. Results and Discussion

2.1. Characterization of CX and ASNase/CX

To confirm the effective immobilization of the enzyme on the material, the CX–OX-600 and the bioconjugate morphology were evaluated by SEM using the optimized ASNase immobilization conditions (0.36 g/L of ASNase, 81 min of contact time, and pH 6.2). According to the SEM micrographs (Figure 1), by comparing the structure of the CX before and after the immobilization with ASNase, the bioconjugate material appears to be much more compact and aggregated. Therefore, it is possible to confirm that ASNase covers the CX's surface almost like the material was coated with the enzyme. These results are useful to verify the successful preparation of the bioconjugate promoted by physical adsorption.

Through TG analysis, we tried to confirm ASNase immobilization onto CX–OX-600. According to Figure 2, in the thermogram of the original CX–OX-600, there was practically no weight loss up to c.a. 500 °C. Above 650 °C, the carbon material was completely gasified. Conversely, the TG profile of the ASNase/CX bioconjugate reveals its first weight loss at about 250 °C, which corresponds to the thermal decomposition of the enzyme. The second weight loss begins at 500 °C and is related to the simultaneous pyrolysis of ASNase and CX. A plateau is reached at a temperature close to 600 °C with 8.7 % of the initial mass remaining until 800 °C, corresponding to the approximate mass content of the enzyme in the bioconjugate. Regarding the DTG profiles, it is possible to observe a decrease in the temperature at which the maximum carbon gasification occurs (from 613 °C and 540 °C for the CX and ASNase/CX, respectively). This shift can be related to the interactions between the amine groups of ASNase and the oxygenated surface groups of the functionalized CX–OX-600 at high temperatures, which may boost carbon gasification.

The changes in the CXs surface upon ASNase immobilization can be confirmed using Raman spectroscopy (Figure 3). There are two primary characteristic bands (D and G) visible in
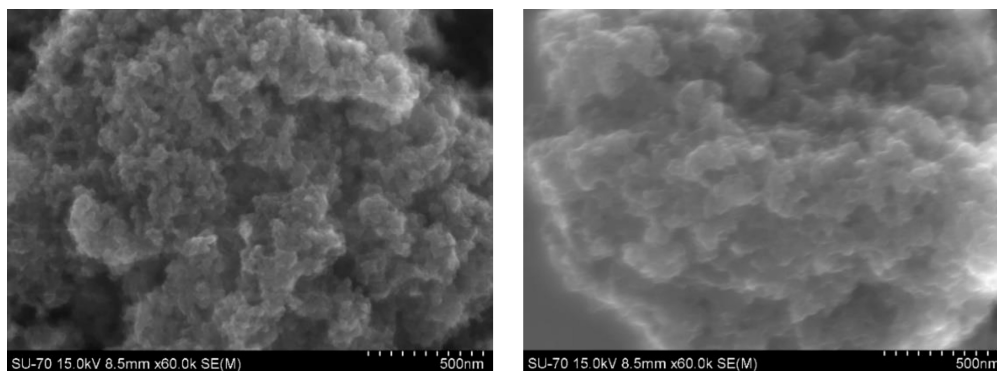
ChemPlusChem

Research Article
doi.org/10.1002/cplu.202400025

Chemistry Europe
European Chemical
Societies Publishing

Figure 1. SEM micrographs of CX–OX-600 (left) and ASNase/CX bioconjugate (right).
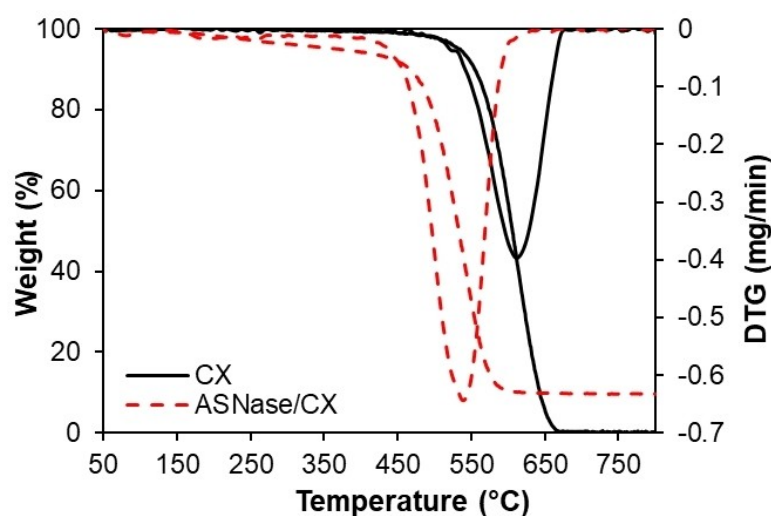

Figure 2. TG and DTG profiles of CX–OX-600 before and after ASNase immobilization.
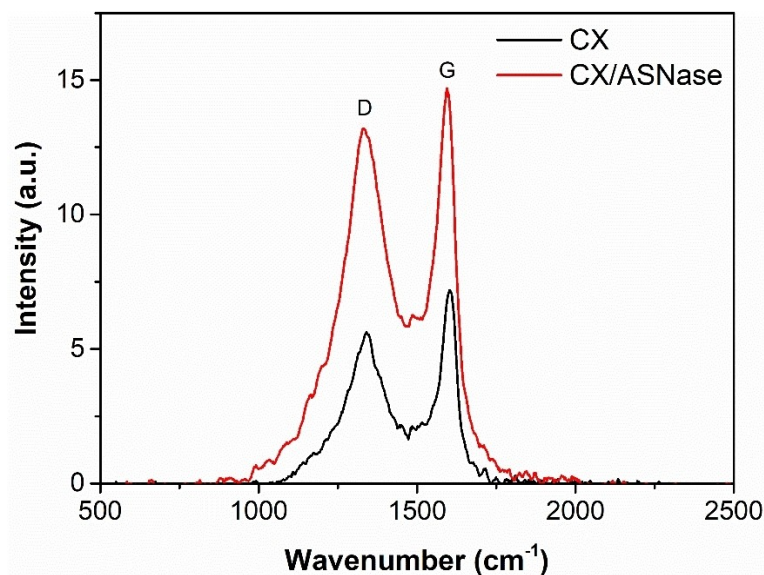

Figure 3. Raman spectra of CX and ASNase/CX bioconjugate.

the spectra of both the CX–OX-600 and ASNase/CX bioconjugate. The ratio of the intensities of the D and G bands (I_D/I_G) is typically used to evaluate the existence of defect sites, the degree of purity in the CXs, and the degree of functionalization.

ChemPlusChem

Research Article
doi.org/10.1002/cplu.202400025

Chemistry Europe
European Chemical
Societies Publishing

For the CX–OX-600 and ASNase/CX bioconjugate, the I_D/I_G values were 0.78 and 0.89, respectively. This increase in the ratio indicates that the CX surface was slightly disturbed by the enzyme immobilization, which increased the degree of disorder and confirmed the correct immobilization.

2.2. Effect of CX surface chemistry on ASNase immobilization and activity

The screening of functionalized CXs for ASNase immobilization was carried out under the optimal conditions obtained in previous studies for pristine CXs (time of contact of 49 min, pH 6.7 and 0.26 g/L of ASNase).[45] However, the *IY* results were shallow for almost all the materials tested under these conditions. These results suggest that too much enzyme was added, saturating the material, and the high activity of the ASNase present in the supernatant masked the activity in the material, translating into null *IY* values. Therefore, it was decided to decrease the ASNase concentration to 0.1 g/L for more reliable screening of the novel materials. Table 1 shows the *RRA* and *IY* results obtained after the immobilization of ASNase onto the different functionalized CXs, under the adjusted conditions mentioned above.

For all the materials used, the *IY* values were always maximum (around 100%), indicating that the concentration of the enzyme solution was fully adsorbed onto the support. However, the attained *RRA* was relatively low for CX–OX and CX–OX-700. In fact, under the conditions studied, none of the functionalized CXs reached *RRA* close to 100%, meaning that these materials could probably adsorb higher enzyme concentrations. The results obtained can be justified by a possible loss of activity during the immobilization process. The process of

adsorption can cause the enzyme to immobilize in such a way that the active centers are not available to react with the substrate, causing mass transfer restrictions.[47] Noma et al. reported the use of p(HEMA–GMA) cryogels for ASNase immobilization with 69.3% of activity recovered and 68.8% of immobilization yield.[48] Similarly, when ASNase was immobilized onto Fe_3O_4@Au nanoparticles, reporting an immobilization yield of 68%.[49]

It should be noted that the functionalization treatments applied to CXs did not significantly change the surface area of the resulting materials (Table 2). The treatment of CXs with HNO_3 results in materials with a high concentration of surface oxygen groups, mostly carboxylic acids, but also lactones, anhydrides, and phenol groups.[50,51] These surface oxygen groups may be quantified by TPD analysis through their decomposition into CO and CO_2 when submitted to specific temperatures.[52] As shown in Table 2, the amount of CO and CO_2 released by each sample is obtained by integrating the Temperature-Programmed Desorption (TPD) spectra (Figures S1 and S2 of the Supporting Information). As expected, the oxidation of CXs drastically increased the number of oxygen functionalities at the material's surface, as the sum of the amount of CO and CO_2 released increased from 216 to 9234 µmol/g for CX and CX–OX, respectively. It can also be observed that CX–OX is the sample with a lower CO/CO_2 ratio, which means that this is the most acidic material, as also confirmed by the pH_{PZC} value of 3.0. The carboxylic acid groups are removed by heating at 400°C, while phenols and carbonyl/quinones remain at the surface of the CX–OX-400 material. An increase in the temperature of the treatment up to 600°C (CX–OX-600) promotes the removal of carboxylic acid and phenolic groups. In comparison, nearly complete removal of surface groups is perceived after treating the CX–OX sample at 700°C (CX–OX-700).[50,51]

FTIR-ATR spectrum of CX was subtracted from the spectrum of the ASNase/CX bioconjugate to validate the presence of ASNase (Figure S3 in the Supporting Information). Both the ASNase and ASNase/CX spectra contain distinctive bands of N–H stretching and bending at 1638 and 1530 cm^{-1}, from amide I and II, respectively.[53] In the region of 1200–800 cm^{-1}, several common bands are seen for ASNase and ASNase/CX bioconjugate, which corresponds to the vibrations of C–C, C–O, C–N, N–H, and C–H bonds in amino acids.[54] However, the typical band corresponding to the aromatic C=C bending of the enzyme in the region of 1700–1500 cm^{-1}[55] is not present in the

Table 1. Screening of functionalized CXs for immobilization of 0.1 g/L of ASNase at pH 6.7 during 49 min of contact time based on the activity per mg of CXs (U/mg), *RRA* and *IY* achieved.

Nanomaterial	Activity (U/mg)	RRA (%)	IY (%)
Pristine CX	0.056 ± 0.002	41 ± 2	99.2 ± 0.3
CX–OX	0.049 ± 0.005	37 ± 4	99.9 ± 0.2
CX–OX-400	0.082 ± 0.003	62 ± 2	99.8 ± 0.1
CX–OX-600	0.086 ± 0.009	65 ± 7	99.7 ± 0.4
CX–OX-700	0.040 ± 0.014	30 ± 10	99.4 ± 0.8

Table 2. CX characterization: surface area (S_{BET}), pH of the point of zero charge (pH_{PZC}) and amounts of CO and CO_2 released obtained by integrating the areas under the TPD spectra.

Materials	S_{BET} (m²/g)	pH_{PZC}	CO (µmol/g)	CO_2 (µmol/g)	CO+CO_2 (µmol/g)	CO/CO_2
Pristine CX	579	6.0	146	70	216	2.1
CX–OX	561	3.0	5167	4067	9234	1.3
CX–OX-400	572	4.5	4700	1708	6407	2.8
CX–OX-600	576	5.2	1500	489	1989	3.1
CX–OX-700	580	5.8	312	91	403	3.4

ChemPlusChem

Research Article
doi.org/10.1002/cplu.202400025

Chemistry Europe
European Chemical
Societies Publishing

ASNase/CX bioconjugate, along with some shifts in the common bands of the 1200–800 cm^{-1} region, which may indicate a possible contribution of aromatic stacking caused by π-π interactions in the immobilization mechanism.

To identify the adsorption mechanism, the analysis of the protonation state and hydrophobicity/hydrophilicity of the ASNase structure was performed (Figure 4). The isoelectric point of ASNase is 5.2.[56] Therefore, at the pH of the aqueous solution used in the adsorption tests (pH 6.7), the surface structure of ASNase II is charged mainly by positive charges of amino acids (arginine, lysine and N-terminus) (Figure 4A). However, glutamic acid, aspartic acid and C-terminus are negatively charged and may contribute to the adsorption process. The hydrophobic/hydrophilic surface of ASNase II is depicted in Figure 4B. According to the results, the contribution of hydrophobic amino acids (alanine, glycine, leucine, valine, proline, isoleucine, methionine, tryptophan and phenylalanine) is to provide structural stability of ASNase. In addition, cysteine contributes to disulfide bridges promoting ASNase folding. Thus, the hydrophilic amino acids (threonine, glutamine, asparagine and serine) are more exposed to interact with CXs.

Since the CXs displayed different treatments, the surfaces will present different interactions with the ASNase II. The Pristine CX and CX−OX-700, which showed low *RRA*, are the materials with the highest hydrophobicity. The absence of treatment on pristine CX leads to the absence of functional groups on the material surface. On the other hand, heat treatment at higher temperatures leads to the almost complete removal of functional groups. Therefore, these CXs primarily interact by hydrophobic, Van der Waals and π-π stacking interactions. The CX−OX, which displays the highest number of functional groups, interacts with ASNase mainly by electrostatic interactions between the negatively charged groups of CX−OX with ASNase guanidinyl group (arginine) and ε-amino group (lysine and N-terminus). The electrostatic interaction leads to relatively weak adsorption due to the repulsion promoted by negatively charged amino acids, which can contribute to this behavior even in a smaller presence. The *RRA* of ASNase immobilized in this support is also low. The CX−OX-400 and CX−OX-600 exhibited the highest *RRA* (62±2% and 65±7%, respectively). However, the CXs materials display different surface characteristics that can determine the adsorption stability of ASNase/CX bioconjugate. The CX−OX-400 presents more functional groups at the CX surface and lower hydrophobicity.

On the other hand, CX−OX-600 shows the opposite. Despite presenting similar *RRA* values, the presence of functional groups charged in excess could lead to easiest ASNase leaching and reduce the possibility of promising operational stability using CX−OX-400, by repulsion of negatively charged amino acids, and leading to a lower possibility of reuse of the ASNase/CX bioconjugate. Thus, CX−OX-600 lower number of functional groups and higher hydrophobicity promotes a balance of interactions (electrostatic and hydrophobic) favorable to operational stability and higher activity of adsorbed ASNase.

Overall, considering the balance between the *RRA* and *IY* (Table 1) and adsorption interactions of ASNase/CX bioconjugate, CX−OX-600 may be regarded as the most promising material, and, for this reason, it was selected as support for the optimization of the immobilization of commercial ASNase through a CCD experimental plan. Finally, as the *IY* values were maximum for all the materials tested, it was decided that the CCD of experiments would be primarily useful for optimizing the *RRA* of the immobilized ASNase.

To further explore the immobilization mechanism, the influence of the ionic strength of the buffer solution on the adsorption of the enzyme to the material was studied. The decrease in the ionic strength of the buffer resulted in a brutal decrease in the *IY* (from 100% to 12%), which indicated the significant influence of hydrophobic interactions between the enzyme and the support on the immobilization process, confirming the previously obtained results.
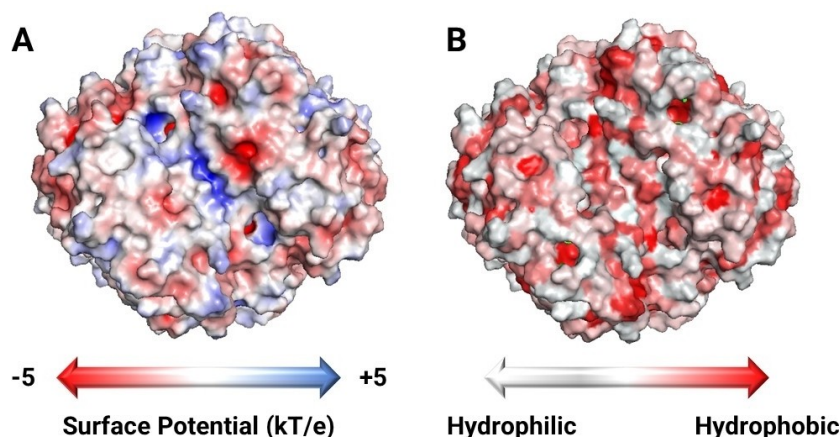

Figure 4. 3D surface of ASNase II structure (PDB: 3ECA) at pH 6.7: (A) Electrostatic charge surface (minimum (−5 kT/e, red) and maximum (5 kT/e, blue) surface potential), (B) Hydrophobic/Hydrophilic surface (red – hydrophobic amino acids, white – hydrophilic amino acids).

2.3. Improvement of immobilization conditions – CCD of experiments

The CCD is a valuable experimental tool in RSM that allows the creation of a second-order model for the dependent variable without the need for a complete three-factorial experiment.[57] This method is very helpful since it allows the analysis of different parameters simultaneously, extending the evaluation to a wider range of possible combinations between the variables and decreasing the number of necessary tests.

The enzyme/support contact time is thought to have an impact on the efficiency of enzymatic immobilization onto support because it influences the likelihood of interactions among the enzyme and the adsorption sites at the surface of the support,[58] as well as the pH of the solution, since it defines the superficial charges and, hence, influences the affinity between the enzyme and the CXs.[59] ASNase concentration is also an important parameter to evaluate since it determines the amount of enzyme the support can adsorb. As a result, a CCD experimental approach was used to evaluate the influence of these variables on the *RRA* of the immobilization process. Table S1 of the Supporting Information shows the levels of each variable, as well as the *RRA* experimental outcomes for all 19 studies conducted.

Using the experimental values obtained, a second-order polynomial model (Equation S1 on the Supporting Information) was fitted to the results and presented in terms of coded factors X_1, X_2, X_3 (time, pH, and enzyme concentration, respectively), translated by Eq. 1.

$$Y = -450.38 - 0.15X_1 + 154.94X_2 + 473.47X_3 - 0.09X_1X_2 - 3.69X_1X_3 + 26.61X_2X_3 + 0.01X_1^2 - 12.63X_2^2 - 469.45X_3^2 \tag{1}$$

Analysis of variance (ANOVA) and Pareto chart were used as valuable tools to evaluate the statistical significance of the polynomial model obtained. The significance of the coefficients was determined by a *p*-value test, considering 95% confidence.

Coefficients of high significance ($p < 0.05$) are highlighted in red in Table S2 of the Supporting Information.

The Pareto chart makes it simple to see the statistically significant impacts of each component on the answer. The impacts on the right of the divisor line are significant and are ranked from largest to smallest (Figure 5).

The strong relevance of enzyme concentration (X_3) on *RRA* value indicates that this parameter is the most important for the efficacy of ASNase immobilization onto CXs. This factor indicates the amount of ASNase accessible for adsorption on the surface of CXs. The low significance of the pH is related to the similarity between the isoelectric point (*pI*) of ASNase (5.2[56]) and the pH_{PZC} of the CX–OX-600 (5.2 – Table 2), showing, once again, that electrostatic interactions do not affect this immobilization procedure. It was anticipated that longer periods of immobilization would result in increased *RRA*. Nevertheless, within the range of values studied), the contact time between the enzyme and the support did not have a significant impact on ASNase immobilization.

2.3.1. Response surface methodology

The response surface plots (Figure 6) show the relationship between two factors and the achieved *RRA* for ASNase immobilization onto CX–OX-600, while the third factor was maintained constant (central value). Specifically, Figures 6a, 6b and 6c, illustrate the surface plots as a function of pH and time, ASNase concentration and time, and ASNase concentration and pH, respectively.

From Figures 6a, it is possible to conclude that the maximum *RRA* is reached for pH values around the central value (pH 6), whereas, at these conditions, *RRA* values of 100% are only touched for times of contact above 100 min. Moreover, it is also possible to observe that *RRA* minimum values are reached at contact times between 20–80 min and at pH values between 4.0–4.5 and 7.5–8.0. Comparing the factors pH and
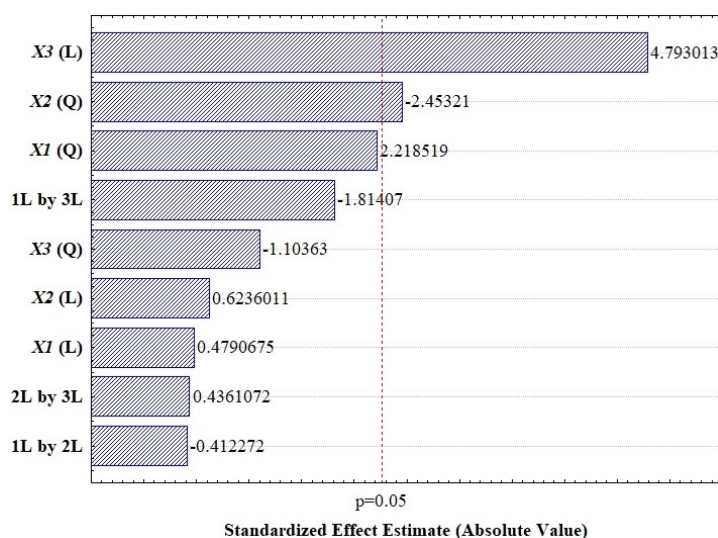

Figure 5. Pareto charts of standardized effects of CCD for ASNase immobilization onto CX–OX-600.

ChemPlusChem

Research Article
doi.org/10.1002/cplu.202400025

Chemistry Europe
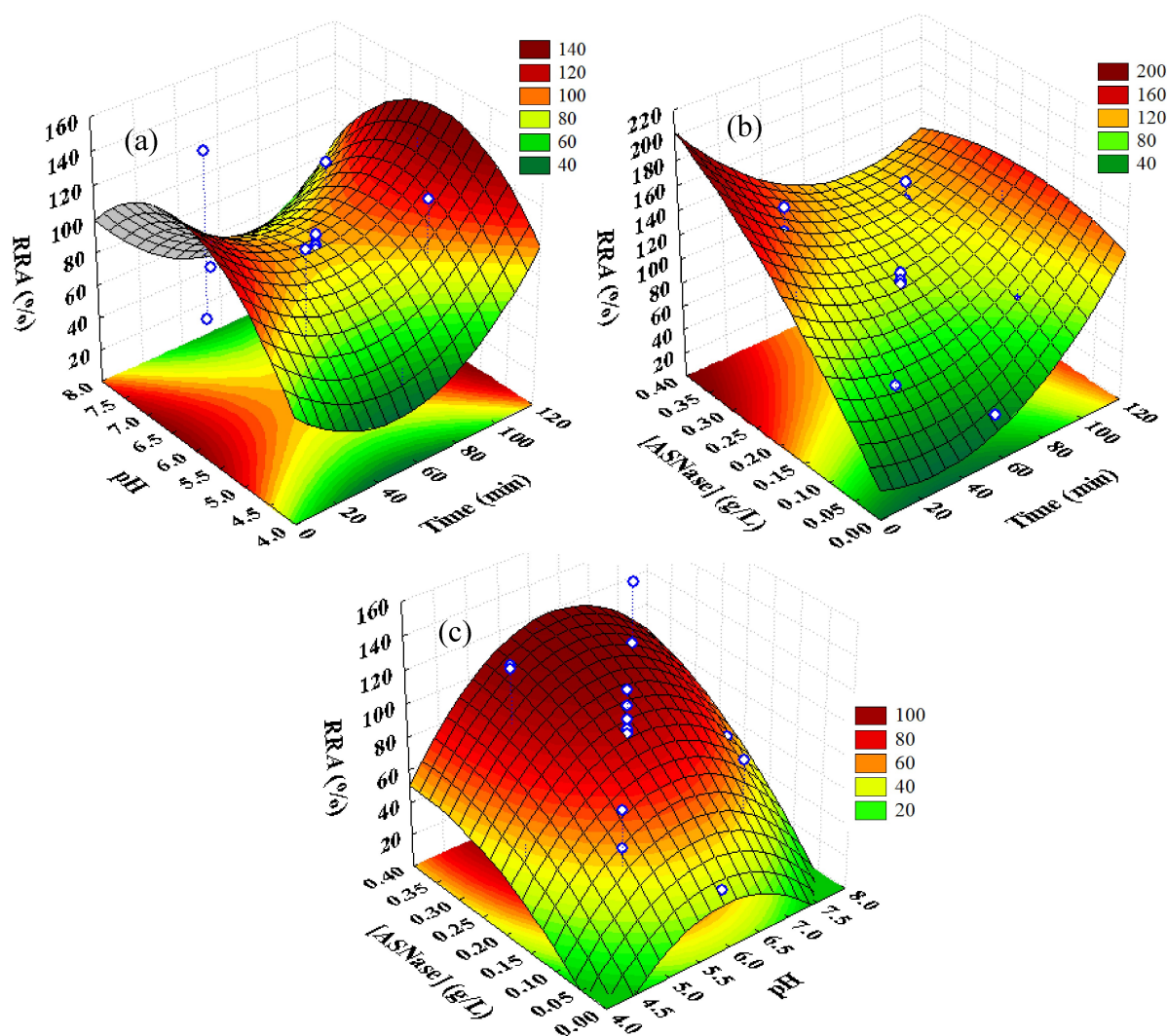European Chemical
Societies Publishing

Figure 6. Response surface plots for *RRA* of immobilized ASNase over CX–OX-600 as a function of: (a) pH and time with an enzyme concentration of 0.2 g/L, (b) enzyme concentration and time at a pH of 6, and (c) enzyme concentration and pH, with a time of contact of 60 min.

contact time, the pH proved to have a higher influence on the *RRA* since the bigger the surface curvature, the higher the significance of the parameter. However, from Figure 6a, it is not possible to predict the optimal conditions of immobilization, which indicates that the optimum conditions are found for another ASNase concentration.

Figure 6b shows that the *RRA* increases with high ASNase concentration for any contact time value. So, minimum *RRA* values are obtained at low contact times (0–40 min) and enzyme concentrations (0–0.05 g/L), while maximum values are obtained at low contact times (0–20 min) and high ASNase concentrations (0.30–0.40 g/L). Therefore, it is possible to conclude that the ASNase concentration contributes more significantly to the response (*RRA*) than the contact time between enzyme and substrate, given the steeper slope of the straight line relative to this factor.

Figure 6c indicates that for any pH value, the higher the ASNase concentration, the higher the *RRA*. As the ANOVA data shows, the enzyme concentration is the most significant

parameter. In this plot, it is already possible to see a value close to the optimum, with maximum values obtained at more neutral pH values (6.0–7.0) and high ASNase concentration values (0.30–0.40 g/L).

2.3.2. Critical relative recovered activity and model validation

As mentioned before, the experimental design and the statistical analysis only considered the *RRA* values as the *IY* remained unchanged throughout the different experiments, ranging from 99.4% to 99.9%. Hence, the CCD methodology facilitated the prediction of the critical values for each parameter that corresponds to the highest *RRA* achievable for optimizing ASNase immobilization onto functionalized CXs. The results indicate that with a time of contact of 81 min, at pH 6.2 and with an ASNase of 0.36 g/L (optimum conditions), the predicted *RRA* of ASNase immobilized onto CX–OX-600 is 111%. The adequacy of the proposed model was evaluated by

ChemPlusChem

Research Article
doi.org/10.1002/cplu.202400025

Chemistry
Europe
European Chemical
Societies Publishing

performing new experiments of ASNase immobilization over functionalized CX–OX-600 in triplicate at the predicted optimum conditions. Under those experimental conditions, an *RRA* of $103 \pm 2\%$ and *IY* of 100% were achieved, which is in good agreement with the ones predicted by the CCD, validating the adequacy of the proposed model. Comparing these results with the ones obtained during the immobilization of ASNase over pristine CXs with a similar pore radius, where, under the optimal conditions of immobilization (116 min of contact time, pH 5.2, ASNase 0.19 g/L), an *RRA* of 85% and an *IY* of 100% were reached,[45] is it possible to conclude that the functionalization of CXs allowed the increase of the enzymatic loading capacity of the support (since the optimal concentration of adsorbed ASNase is higher), increasing the *RRA* achieved. Moreover, the results obtained in this work are also promising when compared to those reported by Almeida et al.,[39] regarding the use of functionalized multi-walled carbon nanotubes (MWCNTs), with *IY* and *RRA* of commercial immobilized ASNase around 95%.

2.4. Characterization of the bioconjugate ASNase/CX

2.4.1. Operational, storage and pH stabilities

The operational stability of ASNase/CX bioconjugate was evaluated throughout 6 cycles of L-Asn hydrolysis and represented in terms of activity per mg of CX (U/mg) after each cycle (Figure 7). After 6 cycles, using CX–OX-600 as immobilization support allowed ASNase to retain 97% of its original activity (0.129 U/mg), displaying exceptional operational stability. The functionalization of CXs promoted the balance between the electrostatic and hydrophobic interactions of the bioconjugate, allowing ASNase to maintain its initial activity for practically 6 reaction cycles without loss, as opposed to the 26% loss of activity verified when using pristine CXs where only hydrophobic interactions are present (Figure S4 on the Supporting Information).

Other authors studied the reusability of *E. coli* ASNase immobilized over other functionalized supports and different immobilization methods. For example, after 6 successive reaction cycles at 60 °C, the ASNase covalently immobilized onto graphene oxide functionalized with L-aspartic acid maintained about 50% of its original activity, while when physically absorbed, it retained only about 35% of its initial activity.[60] ASNase covalently immobilized onto functionalized aluminum oxide nanoparticles and titanium oxide nanoparticles preserved approximately 93% and 94% of their initial enzyme activity, respectively, also after 6 consecutive cycles.[61] Moreover, a study by Ulu et al.[62] showed that ASNase entrapped onto calcium–alginate/functionalized multi-walled carbon nanotubes was able to keep approximately 45% of its initial activity after 6 reuses. In turn, the ASNase physically adsorbed onto amino and carboxyl functionalized Fe_3O_4/SiO_2 nanoparticles showed to retain about 88% of its initial activity after 6 reuse cycles,[63] while the absorption onto maltose functionalized magnetic core/shell $Fe_3O_4@Au$ nanoparticles resulted in an operational stability of around 78% after 6 cycles.[64] All these results highlight the promising reusability properties of the functionalized CXs used in this work as support for ASNase immobilization by physical adsorption.

For enzyme immobilization, another important parameter to consider is storage stability. This parameter is important to evaluate the sustained use and economic viability of the immobilization process. The storage stability of free and immobilized ASNase was studied at 4 °C and 25 °C and is presented in Figure 8. After 10 days of incubation, the bioconjugate was able to retain 85% and 91% of its initial activity at 4 °C and 25 °C, respectively. In comparison with the free enzyme, the use of CX–OX-600 as immobilization support allowed ASNase to remain stable over time with no significant activity loss, with the added value adding of being reusable, unlike the free enzyme. Results obtained by Ulu et al.[65] using ASNase covalently bound to pHEMA-starch composites showed that the free and immobilized ASNase preserved 80% and 60% of activity, respectively, after 15 days of storage at 4 °C in dry conditions. At 25 °C, the immobilized ASNase protected 22% of
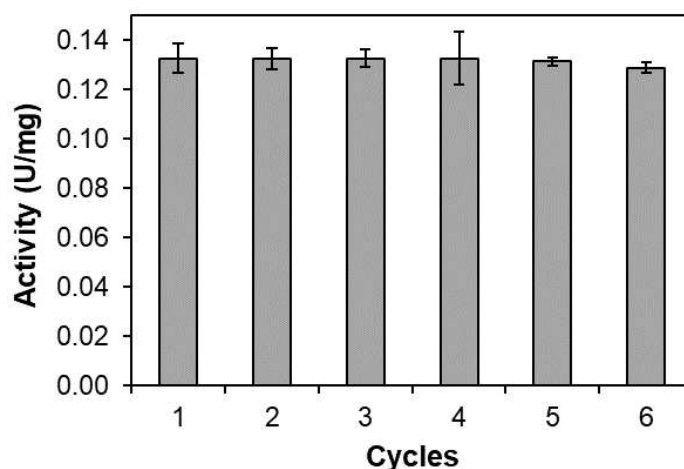

Figure 7. Reusability of 0.36 g/L of immobilized ASNase onto 2 mg of CX–OX-600 at pH 6.2 over 81 min of contact time.
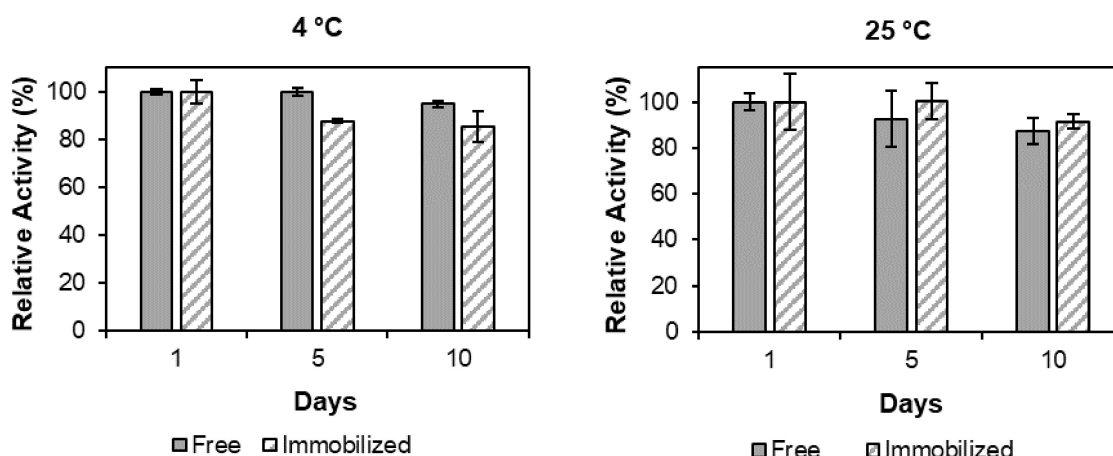
ChemPlusChem

Research Article
doi.org/10.1002/cplu.202400025

Chemistry
Europe
European Chemical
Societies Publishing

Figure 8. Storage stability at 4 °C (left) and 25 °C (right) of free and immobilized ASNase onto CX–OX-600.
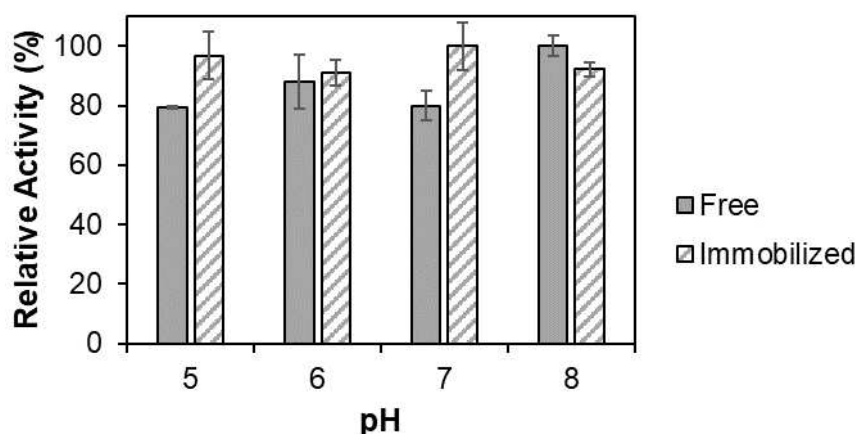

Figure 9. pH stability of free and immobilized ASNase onto CX–OX-600 for an incubation time of 120 min.

its initial activity. Considering that the use of covalent bonds for the immobilization procedure is responsible for stronger interactions between the enzyme and the material, these reported findings highlight the promising results found in this study considering that only a physical adsorption method was employed.

According to the results shown in Figure 9, the immobilized ASNase showed almost no activity loss in the range of pH studied, being more stable at pH 7, while the free enzyme showed a slight decrease in activity at more acidic pH values. Even though there was no significant activity decrease in any case, the immobilized enzyme proved to be more stable in a wider range of pH, highlighting the ability of CX–OX-600 to protect ASNase through a simple yet very efficient physical adsorption interaction.

2.4.2. Kinetic parameters

The kinetic parameters obtained for free and immobilized ASNase are summarized in Table 3. The results suggest a 1.25-

Table 3. Hill kinetic parameters obtained of free and immobilized ASNase (0.36 g/L) onto CX–OX-600 by physical adsorption.

	Free ASNase	Immobilized ASNase
v_{max} (mM/min)	0.40	0.34
S_{50} (mM)	251	314
h	1.7	1.9
k_{cat}/S_{50} (mM^{-1} min^{-1})	0.011	0.012

fold increase in the immobilized enzyme affinity for the substrate. That is most likely due to the immobilized enzyme's better conformational changes (greater cooperativity), which results in increased availability of the active sites and higher affinity for L-Asn, like when ASNase was immobilized onto pristine CXs (Figure S5 on the Supporting Information). If h were equal to one, the Hill equation (shown in the Experimental Section) would reduce to the Michaelis-Menten equation. Positive cooperativity is shown by h values higher than one, which was the case in this work. This suggests that binding one substrate molecule causes conformational changes in the

ChemPlusChem

Research Article
doi.org/10.1002/cplu.202400025

Chemistry Europe
European Chemical
Societies Publishing

enzyme, increasing the affinity at other sites. As a point of comparison, Tarhan et al.[64] reported a 1.86-fold K_M decrease after the physical adsorption of ASNase onto Fe_3O_4@Au nanoparticles, Noma et al.[66] a 2.13-fold K_M decrease with the use of L-asparaginase@hybrid nanoflowers, and Dik et al.[67] a 1.46-fold K_M decrease after the physical adsorption of ASNase onto magnetic nanoparticles. However, the decrease in v_{max} values after immobilization has been frequently reported for ASNase immobilized by physical adsorption,[64,67] and it might be explained by the greater mass transfer limitation of the diffusion layer that surrounds the ASNase particles[68] and by localized charges changes near the active sites of the enzyme,[69] which limit substrate diffusion towards the ASNase/CX bioconjugate. The calculated kinetic parameters translate into relatively similar catalytic efficiencies (k_{cat}/S_{50}) of the free and immobilized ASNase. Furthermore, the obtained Hill coefficients show that both forms of the enzyme exhibit allosteric behavior with positive cooperativity, as already verified when the immobilization of ASNase onto pristine CXs was studied (Table S3 on the Supporting Information). Figure 10 shows the Hill equation fitting to the experimental data.

3. Conclusions

A simple physical adsorption approach was shown to be an effective method for the immobilization of commercial ASNase onto functionalized CXs. With good model accuracies and useful data on the impact of the variable and their interactions, the CCD was an excellent tool for optimizing the immobilization conditions. As opposed to the minor influence of pH and contact time, the variable with the highest impact on immobilization efficiency was ASNase concentration. Under the ideal conditions (contact time of 81 min, ASNase concentration of 0.36 g/L, pH of 6.2), CX–OX-600 was the support that provided the most favorable characteristics for ASNase immobilization, with remarkable *RRA* and *IY* values of 100%. Compared to the native form, one of the key benefits of using immobilized

enzymes in biotechnological approaches is their ability to be reused. The adsorption onto functionalized CX–OX-600 allowed an excellent ASNase operational stability, preserving 97% of its initial activity after 6 continuous reaction cycles. Furthermore, the observed kinetic constants show that the immobilized enzyme has a 1.25-fold higher affinity for the substrate than the free enzyme. The results reveal that CXs are promising supports for ASNase immobilization and that their functionalization is an exciting upgrade, especially for improved enzyme stabilities. The practical application of the immobilized enzyme is crucial to evaluate its feasibility and effectiveness in various fields such as biocatalysis, the food industry, pharmaceuticals, environmental remediation, and biosensors. This evaluation normally focuses on several key aspects, such as catalytic activity, stability, reusability, operational stability, substrate specificity and selectivity, and cost-effectiveness. Another important aspect of an enzyme, mainly to the pharmaceutical industry, is biodisponibility which refers to the extent to which these enzymes are available and active within a given system. The immobilization process can improve the accessibility and activity of the enzymes making them more bioavailable. Therefore, although practical applications were not evaluated in the present work, these discoveries make a valuable contribution towards identifying a simpler and more cost-effective process for immobilization which can be employed in various fields and future studies regarding enzyme-immobilized biodisponibility is one of our future targets.

Experimental Section

Enzyme and reagents

Lyophilized and purified recombinant ASNase from *E. coli* ASI.357[70] ($\geq$96.0%, P1321-10000; 10000 IU) with a specific activity of 225 IU/mg and without any additives was provided by Deltaclon S.L., Spain. One IU of ASNase is defined as the amount of enzyme required to generate 1 μmol of ammonia per minute at pH 8.6 and 37°C. L-Asn ($\geq$99.0%), disodium hydrogen phosphate ($\geq$99.0%) and tris(hydroxymethyl)aminomethane (TRIS) ($\geq$99.0%) were ac-
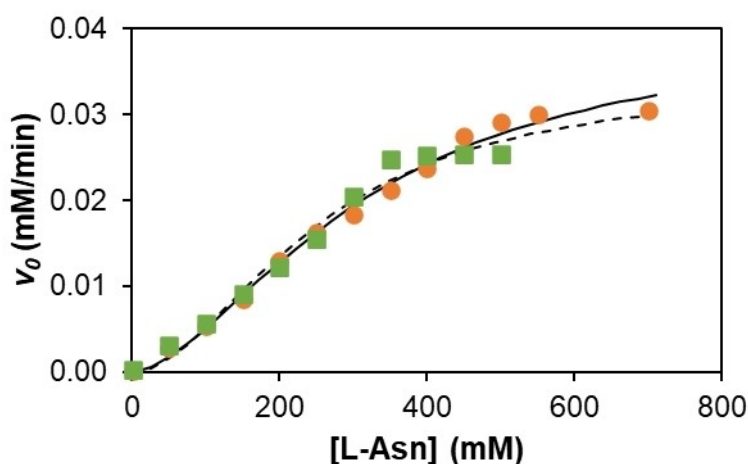

Figure 10. Initial reaction rates (v_0) of free ( ) and immobilized ( ) ASNase (0.36 g/L) onto CX–OX-600 by physical adsorption. The solid (free) and dashed (immobilized) lines represent the fit of the experimental data to the Hill equation.

ChemPlusChem

Research Article
doi.org/10.1002/cplu.202400025

Chemistry
Europe
European Chemical
Societies Publishing

quired from VWR International, LLC. Trichloroacetic acid (TCA) ($\geq$ 99.0%) was bought from J.T. Baker, while citric acid ($\geq$ 99.5%) and Nessler's reagent (dipotassium tetraiodomercurate (II)) were obtained by Merck Chemical Company (Germany). Sigma-Aldrich provided sodium hydroxide ($\geq$ 98.0%) and hydrochloric acid (37%).

Synthesis and characterization of CXs

The CXs were initially synthesized through the polycondensation of formaldehyde and resorcinol at pH 6, resulting in CXs with an average pore diameter of 12 nm, as described in earlier publications.[40,45] Later, these materials were functionalized by hydrothermal oxidation with nitric acid (CX—OX) and subsequently treated at different temperatures under a nitrogen flow: 400°C (CX—OX-400), 600°C (CX—OX-600) and 700°C (CX—OX-700), according to the procedure described in detail elsewhere.[71]

N_2 adsorption-desorption at -196°C allowed to determine CXs textural properties by using a Quantachrome NOVA 4200e apparatus. The specific surface areas (S_{BET}) were calculated by Brunauner-Emmett-Teller (BET) from N_2 adsorption in the relative pressure range from 0.05 to 0.15.

A Hitachi SU-70 high-resolution field emission scanning electron microscope (HR-FESEM) running at 15 kV was used to obtain the structural characterization of the CX and ASNase/CX bioconjugate.

Thermogravimetric (TG) analyses were performed using an STA 490 PC/4/H Luxx 134 Netzsch thermal analyzer. In each experiment, approximately 10 mg of the sample was loaded onto a crucible. The sample was then heated at a rate of 10°C per minute, ranging from 50°C to 800°C under a continuous airflow, while monitoring and recording the weight continuously.

Raman spectra were obtained using a WITec alpha300 R-Confocal Raman Imaging Microscope with a laser wavelength of 532 nm and 1 mW power.

To obtain pore size distribution curves and cumulative pore volume, the BJH method was employed on the desorption branch. TPD was used to characterize and quantify the surface chemical groups. The samples were heated at a rate of 5°C min^{-1} until 1100°C under helium flow using an AMI-300 Catalyst Characterization Instrument (Altamira Instruments) equipped with a quadrupole mass spectrometer (Ametek, Mod. Dymaxion). By integration of the TPD spectra, the total amount of CO and CO_2 evolved from the samples were obtained. Additionally, the pH of the point of zero charge (pH_{PZC}) of the different materials was calculated according to a drift method suggested in the literature.[72]

FTIR was performed to compare the spectra (2000–700 cm^{-1}) of ASNase and ASNAse/CX. The analyses were performed using 256 scans with a resolution of 4 cm^{-1} in a JASCO FT/IR-6800 spectrometer (JASCO Analytical Instruments, USA) equipped with a MIRacleTM Single Reflection ATR (attenuated total reflectance ZnSe crystal plate) accessory (PIKE Technologies, USA).

ASNase immobilization over functionalized CXs

The physical adsorption of ASNase onto functionalized CXs was studied by adding 200 μL ASNase solution (from 0.02 to 0.38 g/L, or 4.5 to 85.5 IU/mL) prepared in an appropriate citrate/phosphate buffer (50 mM) at different pH values to 2 mg of each CX. The mixtures were agitated at 50 rpm in a vertical mini rotator (Grant Instruments Lda., model PTR-35) before being centrifuged at 100 g for 6 min. A control using free ASNase was made for each experimentally tested condition.

A CCD was used to optimize the experimental parameters (contact time, pH, and ASNase concentration).

ASNase activity measurement

The reaction between the enzyme (ASNase) and the substrate (L-Asn) defines the enzyme's specific activity. The amount of product created (ammonium) is then used to calculate the extension of the reaction using the Nessler technique. The Nessler method is a simple, quick, and inexpensive approach to quantify the ammonium in solution, and the FDA approves it for pure ASNase formulations.[73] The characteristic yellow-to-brown reaction mixture resulting from the reaction between Nessler reagent and ammonium can be quantified by spectrophotometry at 436 nm.[73] For this, a calibration curve was made beforehand, using ammonium sulfate.

The experimental procedure has been previously reported in detail elsewhere[45] and involves the addition of enzyme solution or ASNase/CX bioconjugate to the reaction mixture (50 mM Tris—HCl buffer pH 8.6, 189 mM L-Asn solution, and distilled water), which were then incubated at 37°C for 30 min under stirring. The linearity of the reaction over 30 min under the described conditions has been verified.[74] After incubation, TCA (1.5 M) was used to stop the reaction. The amount of ammonium released was measured by mixing each sample with Nessler's reagent and distilled water and quantified by spectrophotometry at 436 nm (JASCO V-560 UV-Vis spectrophotometer). One unit of ASNase activity (U), for the free enzyme, is equal to the enzyme amount necessary to produce 1 μmol of ammonium per minute at 37°C at pH 8.6. In the case of the immobilized enzyme, it is defined as the quantity of enzyme that produces 1 μmol of ammonium per minute, per unit mass of support, at the same temperature.

Effect of functionalization and optimization of immobilization conditions by experimental design

The effect of the functionalization of CX was evaluated under different conditions (CX—OX, CX-400, CX—OX-600, and CX—OX-700) on the *RRA* and *IY*. The screening of the materials was tested through the immobilization of ASNase onto 2 mg of each of the 6 different types of functionalized CXs under the optimal conditions obtained in previous studies for non-functionalized CX (time of contact of 49 min, pH 6.7 and 0.26 g/L of ASNase). The material that allows higher *RRA* and *IY* was then used to optimize the immobilization conditions by CCD of experiments (detailed explanation in the Supporting Information).

Characterization of free and immobilized ASNase

Operational and storage stability of the immobilized ASNase

To study the reusability of the bioconjugate, 2 mg of ASNase/CX—OX-600 was incubated with the reaction mixture containing L-Asn (189 mM), Tris—HCl buffer (50 mM, pH 8.6), and distilled water, for 30 min, under stirring, at 37°C. At the end of each cycle, a sample was withdrawn, the supernatant was separated from the material, and the enzymatic reaction was stopped with the addition of TCA (1.5 M) to the supernatant. Afterward, the bioconjugate was washed with 1 mL of citrate/phosphate buffer at optimal pH value and resuspended in fresh substrate solution. Each assay was performed in triplicate over the course of 6 successive cycles.

To determine the storage stability, the activities of free and immobilized ASNase were measured after 5 and 10 days of storage

at 4 °C and 25 °C. The immobilized enzyme was stored in 200 μL of citrate/phosphate buffer at optimal pH value. The initial activity was assumed as 100% and the relative activities were calculated by comparison.

pH stability

To evaluate the pH stability, the free and immobilized ASNase were incubated at 25 °C with different buffers (phosphate–citrate buffer 50 mM from pH 5 to 8) for 120 min. The relative activity was calculated from the sample's residual activity to initial activity ratio. For each assay, duplicate runs were made, and the standard deviation was determined.

Kinetic parameters

The kinetic parameters of free and immobilized ASNase onto CX–OX-600 were obtained by measuring ASNase activity with L-Asn as the substrate at 1–700 mM concentrations. CurveExpert software was used to obtain the nonlinear curve fitting of the reaction rate *vs.* L-Asn concentration plot. The kinetic behavior of the reaction followed an allosteric sigmoidal model, which is commonly characterized by the Hill equation (Eq. 2):

$$v = \frac{v_{max}[S]^h}{(S_{50})^h + [S]^h} \qquad (2)$$

where S_{50} measures the enzyme affinity to the substrate (equivalent to the K_m parameter in the Michaelis-Menten equation) and the parameter h describes the degree of cooperativity. The k_{cat} (turnover number) to S_{50} ratio was used to calculate the ASNase efficiency.[75]

Computational analysis

The surface charge and hydrophobicity of *E. coli* ASNase II were analyzed using PDB: 3ECA. ASNase II protonation state was analyzed using ProteinPrepare (PlayMolecule web server – playmolecule.org).[76] The PDB file was downloaded from the Protein Data bank and uploaded to the ProteinPrepare application. The pK_a calculation was performed at pH 6.7, with no water molecules and ligands from the input PDB file. The protonated PDB file and protonation table were downloaded and assessed after calculation. The electrostatic surface was calculated using automatically configured sequentially focusing multigrid calculation on Adaptive Poisson-Boltzmann Solver (APBS), and surface hydrophobicity was estimated by Eisenberg's scale.[77] Both surfaces were created using PyMOL Molecular Graphics System, Version 2.5.2 Schrödinger, LLC.

Author Contributions

R.A.M.B., R.O.C., I.G.C., M.A.B.: Methodology, Investigation. M.M.P.: Computational analysis. R.A.M.B. and R.O.C.: Writing – original draft. S.A.C.C., M.G.F., J.L.F., V.C.S.-E., A.P.M.T., and C.G.S.: Methodology, Investigation, Funding acquisition, Resources, Writing – review and editing. A.P.M.T. and C.G.S.: Supervision. All authors have read and agreed to the published version of the manuscript.

Conflict of Interests

The authors declare no conflict of interest.

Data Availability Statement

The data that support the findings of this study are available from the corresponding author upon reasonable request.

Keywords: Adsorption · Bioconjugate · Functionalized carbon xerogels · Immobilization · L-asparaginase

[1] R. Masetti, A. Pession, *Biologics* **2009**, *3*, 359–368.
[2] World Health Organization, "Childhood cancer," can be found under https://www.who.int/news-room/fact-sheets/detail/cancer-in-children, **2021**.
[3] M. M. O'Brien, A. E. Seif, S. P. Hunger, *Wintrobe's Clinical Hematology: Fourteenth Edition* **2018**, ■■■ Dear Author, if the journal has volumes, please add the journal number■■■4939–5015.
[4] N. V. Frey, S. M. Luger, *Blood* **2015**, *126*, 589–596.
[5] S. Kumar, V. Venkata Dasu, K. Pakshirajan, *Bioresour. Technol.* **2011**, *102*, 2077–2082.
[6] G. Shakambari, B. Ashokkumar, P. Varalakshmi, *Biocatal. Agric. Biotechnol.* **2019**, *17*, DOI 10.1016/j.bcab.2018.11.018.
[7] D. Killander, A. Dohlwitz, L. Engstedt, S. Franzén, G. Gahrton, B. Gullbring, G. Holm, A. Holmgren, S. Hoglund, A. Killander, D. Lockner, H. Mellstedt, P. J. Moe, J. Palmblad, P. Reizenstein, K.-O. Skarberg, B. Swedberg, A.-M. Úden, B. Wadman, L. Wide, L. Asht, *Cancer* **1976**, *37*, 220–228.

ChemPlusChem

Research Article
doi.org/10.1002/cplu.202400025

Chemistry
Europe
European Chemical
Societies Publishing

[8] M. R. Tabandeh, M. Aminlari, *J. Biotechnol.* **2009**, *141*, 189–195.

[9] F. Xu, M. J. Oruna-Concha, J. S. Elmore, *Food Chem.* **2016**, *210*, 163–171.

[10] S. Zuo, T. Zhang, B. Jiang, W. Mu, *Extremophiles* **2015**, *19*, 841–851.

[11] J. Li, J. Wang, L. G. Bachas, *Anal. Chem.* **2002**, *74*, 3336–3341.

[12] T. Batool, E. A. Makky, M. Jalal, M. M. Yusoff, *Appl. Biochem. Biotechnol.* **2016**, *178*, 900–923.

[13] M. Kozak, S. Jurga, *Acta Biochim. Pol.* **2002**, *49*, 509–513.

[14] H. E. Wade, R. Elsworth, D. Herbert, J. Keppie, K. Sargeant, *Lancet* **1968**, *292*, 776–777.

[15] A. Shrivastava, A. A. Khan, M. Khurshid, M. A. Kalam, S. K. Jain, P. K. Singhal, *Crit. Rev. Oncol. Hematol.* **2016**, *100*, DOI 10.1016/j.critrevonc.2015.01.002.

[16] A. M. Lopes, L. de Oliveira-Nascimento, A. Ribeiro, C. A. Tairum, C. A. Breyer, M. A. De Oliveira, G. Monteiro, C. M. de Souza-Motta, P. de O Magalhães, J. G. F. Avendaño, A. M. Cavaco-Paulo, P. G. Mazzola, C. de O Rangel-Yagui, L. D. Sette, A. Converti, A. Pessoa, *Crit. Rev. Biotechnol.* **2017**, *37*, 82–99.

[17] E. H. Panosyan, N. L. Seibel, S. Martin-Aragon, P. S. Gaynon, I. A. Avramis, H. Sather, J. Franklin, J. Nachman, L. J. Ettinger, M. La, P. Steinherz, L. J. Cohen, S. E. Siegel, V. I. Avramis, *J Pediatr Hematol Oncol* **2004**, *26*, 217–226.

[18] G. A. Kotzia, N. E. Labrou, *J. Biotechnol.* **2005**, *119*, 309–323.

[19] G. A. Kotzia, N. E. Labrou, *J. Biotechnol.* **2007**, *127*, 657–669.

[20] D. Castro, A. S. C. Marques, M. R. Almeida, G. B. de Paiva, H. B. S. Bento, D. B. Pedrolli, M. G. Freire, A. P. M. Tavares, V. C. Santos-Ebinuma, *Appl. Microbiol. Biotechnol.* **2021**, *105*, 4515–4534.

[21] A. Vimal, A. Kumar, *Biotechnol. Genet. Eng. Rev.* **2017**, *33*, 40–61.

[22] D. N. Tran, J. B. Kenneth Jr, *ACS Catal.* **2011**, *1*, 956–968.

[23] B. Singh, *Biotechnology Expanding Horizons*, Kalyani, India, **2009**.

[24] C. Mateo, J. M. Palomo, G. Fernandez-Lorente, J. M. Guisan, R. Fernandez-Lafuente, *Enzyme Microb. Technol.* **2007**, *40*, 1451–1463.

[25] J. M. Bolivar, J. M. Woodley, R. Fernandez-Lafuente, *Chem. Soc. Rev.* **2022**, *51*, 6251–6290.

[26] A. Ulu, B. Ates, *Bioconjugate Chem.* **2017**, *28*, 1598–1610.

[27] Y. Q. Zhang, W. L. Zhou, W. De Shen, Y. H. Chen, X. M. Zha, K. Shirai, K. Kiguchi, *J. Biotechnol.* **2005**, *120*, 315–326.

[28] R. M. Azevedo, J. B. Costa, P. Serp, J. M. Loureiro, J. L. Faria, C. G. Silva, A. P. M. Tavares, *J. Chem. Technol. Biotechnol.* **2015**, *90*, 1570–1578.

[29] A. P. M. Tavares, C. G. Silva, G. Dražić, A. M. T. Silva, J. M. Loureiro, J. L. Faria, *J. Colloid Interface Sci.* **2015**, *454*, 52–60.

[30] J. Zdarta, A. S. Meyer, T. Jesionowski, M. Pinelo, *Catalysts* **2018**, *8*, DOI 10.3390/catal8020092.

[31] L. Wang, L. Wei, Y. Chen, R. Jiang, *J. Biotechnol.* **2010**, *150*, 57–63.

[32] F. L. Oliveira, A. de S França, A. M. De Castro, R. O. M. Alves de Souza, P. M. Esteves, R. S. B. Gonçalves, *ChemPlusChem* **2020**, *85*, 2051–2066.

[33] L. A. Ramírez-Montoya, A. Concheso, I. D. Alonso-Buenaposada, H. García, J. Angel Menéndez, A. Arenillas, M. A. Montes-Morán, *Carbon N Y* **2017**, *118*, 743–751.

[34] M. Kakunuri, S. Vennamalla, C. S. Sharma, *RSC Adv.* **2015**, *5*, 4747–4753.

[35] A. M. Elkhatat, S. A. Al-Muhtaseb, *Adv. Mater.* **2011**, *23*, 2887–2903.

[36] S. A. Al-Muhtaseb, J. A. Ritter, *Adv. Mater.* **2003**, *15*, 101–114.

[37] N. Job, A. Thery, R. Pirard, J. Marien, L. Kocon, J. N. Rouzaud, F. Beguin, J. P. Pirard, *Carbon N Y* **2005**, *43*, 2481–2494.

[38] A. Olusegun, H. A. Makun, I. M. Ogara, M. Edema, K. O. Idahor, B. F. Oluwabamiwo, M. E. Eshiett, *IntechOpen* **2012**, ■■■ Dear Author, if the journal has volumes, please add the journal number■■■DOI 10.1016/j.colsurfa.2011.12.014.

[39] M. R. Almeida, R. O. Cristóvão, M. A. Barros, J. C. F. Nunes, R. A. R. Boaventura, J. M. Loureiro, J. L. Faria, M. C. Neves, M. G. Freire, V. C. Santos-Ebinuma, A. P. M. Tavares, C. G. Silva, *Sci. Rep.* **2021**, *11*, 1–13.

[40] J. P. S. Sousa, M. F. R. Pereira, J. L. Figueiredo, *Catalysts* **2012**, *2*, 447–465.

[41] N. Mahata, M. F. R. Pereira, F. Suárez-García, A. Martínez-Alonso, J. M. D. Tascón, J. L. Figueiredo, *J. Colloid Interface Sci.* **2008**, *324*, 150–155.

[42] A. M. T. Silva, B. F. Machado, J. L. Figueiredo, J. L. Faria, *Carbon N Y* **2009**, *47*, 1670–1679.

[43] D. Hulicova-Jurcakova, M. Seredych, G. Q. Lu, T. J. Bandosz, *Adv. Funct. Mater.* **2009**, *19*, 438–447.

[44] H. P. Boehm, *Carbon N Y* **2002**, *40*, 145–149.

[45] R. A. M. Barros, R. O. Crist, S. A. C. Carabineiro, M. C. Neves, M. G. Freire, J. L. Faria, V. C. Santos-ebinuma, A. P. M. Tavares, G. Silva, *J. Biotechnol.* **2022**, *11*, DOI https://doi.org/10.3390/biotech11020010 Academic.

[46] R. O. Cristovao, M. R. Almeida, M. A. Barros, J. C. F. Nunes, R. A. R. Boaventura, J. M. Loureiro, J. L. Faria, M. C. Neves, M. G. Freire, V. C. Ebinuma-Santos, A. P. M. Tavares, C. G. Silva, *RSC Adv.* **2020**, *10*, 31205–31213.

[47] F. Gashtasbi, G. Ahmadian, K. A. Noghabi, *Enzyme Microb. Technol.* **2014**, *64–65*, 17–23.

[48] S. A. Ali Noma, Ö. Acet, A. Ulu, B. Önal, M. Odabaşı, B. Ateş, *Polym. Test.* **2021**, *93*, DOI 10.1016/j.polymertesting.2020.106980.

[49] T. Tarhan, G. Dik, A. Ulu, B. Tural, S. Tural, B. Ateş, *Top Catal* **2022**, ■■■ Dear Author, if the journal has volumes, please add the journal number■■■DOI 10.1007/s11244-022-01742-y.

[50] J. L. Figueiredo, M. F. R. Pereira, *Catal. Today* **2010**, *150*, 2–7.

[51] J. L. Figueiredo, M. F. R. Pereira, M. M. A. Freitas, J. J. M. Órfão, *Carbon N Y* **1999**, *37*, 1379–1389.

[52] C. G. Silva, A. P. M. Tavares, G. Dražič, A. M. T. Silva, J. M. Loureiro, J. L. Faria, *ChemPlusChem m* **2014**, *79*, 1116–1122.

[53] E. V. Kudryashova, M. V. Pokrovskaya, S. S. Alexandrova, A. A. Vinogradov, N. N. Sokolov, *Anal. Biochem.* **2020**, *598*, DOI 10.1016/j.ab.2020.113694.

[54] M. Mecozzi, E. Sturchio, *J Imaging* **2017**, *3*, DOI 10.3390/jimaging3010011.

[55] A. Barth, *Prog. Biophys. Mol. Biol.* **2000**, *74*, 141–173.

[56] R. O. Cristóvão, R. A. M. Barros, J. G. Pinho, L. S. Teixeira, M. C. Neves, M. G. Freire, J. L. Faria, V. C. Santos-ebinuma, A. P. M. Tavares, C. G. Silva, *Appl. Sci.* **2022**, *12*, DOI https://doi.org/10.3390/app12178924.

[57] N. Ivanova, V. Gugleva, M. Dobreva, I. Pehlivanov, S. Stefanov, V. Andonova, *Intech* **2016**, *i*, 13.

[58] A. M. H. Da Silva, A. P. M. Tavares, C. M. R. Rocha, R. O. Cristóvão, J. A. Teixeira, E. A. MacEdo, *Process Biochem.* **2012**, *47*, 1095–1101.

[59] N. R. Mohamad, N. H. C. Marzuki, N. A. Buang, F. Huyop, R. A. Wahab, *Biotechnol. Biotechnol. Equip.* **2015**, *29*, 205–220.

[60] M. Monajati, S. Borandeh, A. Hesami, D. Mansouri, A. M. Tamaddon, *Chem. Eng. J.* **2018**, *354*, 1153–1163.

[61] S. Agrawal, N. Kango, *Int. J. Biol. Macromol.* **2019**, *135*, 1142–1150.

[62] A. Ulu, M. Karaman, F. Yapıcı, M. Naz, S. Sayın, E. İ Saygılı, B. Ateş, *Catal. Lett.* **2020**, *150*, 1679–1691.

[63] S. A. A. Noma, A. Ulu, S. Koytepe, B. Ateş, *Biocatal. Biotransform.* **2020**, *38*, 392–404.

[64] T. Tarhan, A. Ulu, M. Sariçam, M. Çulha, B. Ates, *Int. J. Biol. Macromol.* **2020**, *142*, 443–451.

[65] A. Ulu, S. Koytepe, B. Ates, *Polym. Bull.* **2016**, *73*, 1891–1907.

[66] S. A. A. Noma, B. S. Yılmaz, A. Ulu, N. Özdemir, B. Ateş, *Catal. Lett.* **2021**, *151*, 1191–1201.

[67] G. Dik, A. Ulu, O. O. Inan, S. Atalay, B. Ateş, *Catal Letters* **2022**, ■■■ Dear Author, if the journal has volumes, please add the journal number■■■DOI 10.1007/s10562-022-04075-3.

[68] F. Gashtasbi, G. Ahmadian, K. A. Noghabi, *Enzyme Microb. Technol.* **2014**, *64–65*, 17–23.

[69] H. Torabizadeh, A. Mahmoudi, *Biotechnol. Rep.* **2018**, *17*, 97–103.

[70] M. T. Q. de Magalhães, T. S. de Araújo, B. M. Silva, L. P. Icart, S. M. N. Scapin, M. da Silva Almeida, L. M. T. R. Lima, *Biophys. Chem.* **2023**, *299*, DOI 10.1016/j.bpc.2023.107041.

[71] S. A. C. Carabineiro, T. Thavorn-Amornsri, M. F. R. Pereira, J. L. Figueiredo, *Water Res.* **2011**, *45*, 4583–4591.

[72] J. Rivera-Utrilla, I. Bautista-Toledo, M. A. Ferro-Garca, C. Moreno-Castilla, *J. Chem. Technol. Biotechnol.* **2001**, *76*, 1209–1215.

[73] A. Magri, M. F. Soler, A. M. Lopes, E. M. Cilli, P. S. Barber, A. Pessoa, J. F. B. Pereira, *Anal. Bioanal. Chem.* **2018**, *410*, 6985–6990.

[74] C. Lanvers, J. Paulo, V. Pinheiro, G. Hempel, G. Wuerthwein, J. Boos, *Anal. Biochem.* **2002**, *309*, 117–126.

[75] R. A. Copeland, in *Enzymes (Essen)*, **2000**.

[76] G. Martínez-Rosell, T. Giorgino, G. De Fabritiis, *J. Chem. Inf. Model.* **2017**, *57*, 1511–1516.

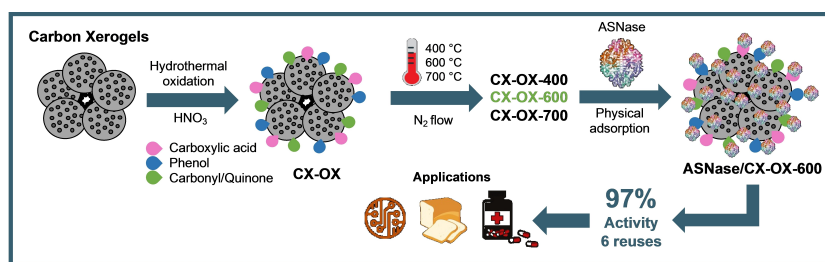[77] D. Eisenberg, E. Schwarz, M. Komaromy, R. Wall, *J. Mol. Biol.* **1984**, *179*, 125–142.

RESEARCH ARTICLE

R. A. M. Barros, R. O. Cristóvão, I. G. Carneiro, M. A. Barros, M. M. Pereira, S. A. C. Carabineiro, M. G. Freire, J. L. Faria, V. C. Santos-Ebinuma, A. P. M. Tavares, C. G. Silva*

1 – 14

Improved L-Asparaginase properties and reusability by immobilization onto functionalized carbon xerogels

The development of an efficient strategy for immobilizing L-asparaginase enzyme onto functionalized carbon xerogels is the focus of this work. The results reveal the importance of tuning the surface chemistry of the materials and prove the enhanced activity, higher affinity with the substrate, and reusability of L-asparaginase achieved through immobilization.

SPACE RESERVED FOR IMAGE AND LINK

Share your work on social media! *ChemPlusChem* has added Twitter as a means to promote your article. Twitter is an online microblogging service that enables its users to send and read short messages and media, known as tweets. Please check the pre-written tweet in the galley proofs for accuracy. If you, your team, or institution have a Twitter account, please include its handle @username. Please use hashtags only for the most important keywords, such as #catalysis, #nanoparticles, or #proteindesign. The ToC picture and a link to your article will be added automatically, so the **tweet text must not exceed 250 characters**. This tweet will be posted on the journal's Twitter account (follow us @ChemPlusChem) upon publication of your article in its final form. We recommend you to re-tweet it to alert more researchers about your publication, or to point it out to your institution's social media team.

ORCID (Open Researcher and Contributor ID)

Please check that the ORCID identifiers listed below are correct. We encourage all authors to provide an ORCID identifier for each coauthor. ORCID is a registry that provides researchers with a unique digital identifier. Some funding agencies recommend or even require the inclusion of ORCID IDs in all published articles, and authors should consult their funding agency guidelines for details. Registration is easy and free; for further information, see http://orcid.org/.

Maria A. Barros
Matheus M. Pereira
Mara G. Freire
Sónia A. C. Carabineiro
Joaquim L. Faria
Raquel O. Cristóvão
Inês. G. Carneiro
Rita A. M. Barros
Cláudia G. Silva
Valéria C. Santos-Ebinuma
Ana P. M. Tavares